frontiers | Frontiers in Materials

TYPE Original Research
PUBLISHED 17 October 2023
DOI 10.3389/fmats.2023.1277634

OPEN ACCESS

EDITED BY
Derun Zhang,
Huazhong University of Science and Technology, China

REVIEWED BY
Wensheng Wang,
Jilin University, China
Yiming Li,
Northeast Forestry University, China
Hui Chen,
Texas A&M University, United States

*CORRESPONDENCE
Shuang Sun,
sunshuang@jlju.edu.cn

RECEIVED 15 August 2023
ACCEPTED 19 September 2023
PUBLISHED 17 October 2023

CITATION
Shi C, Wang J, Sun S, Lv D, Xu L and Zhang S (2023), Research on properties of basalt fiber-reinforced asphalt mastic. *Front. Mater.* 10:1277634. doi: 10.3389/fmats.2023.1277634

Research on properties of basalt fiber-reinforced asphalt mastic

Chenglin Shi[1], Jianan Wang[1,2], Shuang Sun[1]*, Dongye Lv[3], Lina Xu[1] and Sufeng Zhang[4]

[1]School of Transportation Science and Engineering, Jilin Jianzhu University, Changchun, China, [2]CCCC Comprehensive Planning and Design Institute Co., Ltd., Beijing, China, [3]Transportation Information and Communication Center, Department of Transportation of Jilin Province, Changchun, China, [4]Heilongjiang Highway Construction Center, Harbin, China

A basalt fiber-reinforced asphalt mixture can improve the engineering properties of asphalt pavement and prolong the service life of the road. However, few studies have systematically examined the composition of asphalt mixtures or the optimal ratio of fiber asphalt mastic suitable for different structural types. The effects of fiber content, filler–asphalt ratio, and asphalt viscosity on the properties of fiber asphalt mastic were investigated by orthogonal experiments to explore the reinforcement effect of basalt fiber on asphalt mastic. The optimal ratio of fiber asphalt mastic suitable for gap-graded and dense-graded asphalt mixtures was obtained by the fuzzy comprehensive evaluation (FCE) method. Meanwhile, the reinforcement effects of bundled basalt fiber (BBF), flocculated basalt fiber (FBF), polyester fiber (PF), and lignin fiber (LF) on asphalt mastic were compared and analyzed based on the optimal ratio of FBF asphalt mastic. The results showed that the optimal fiber asphalt mastic ratio suitable for gap-graded and dense-graded asphalt mixtures were that fiber content, filler–asphalt ratio, and asphalt viscosity were 3%, 1.8, and 1.1 Pa·s and 2%, 1.0, and 0.7 Pa·s, respectively. Analyzing the properties of different types of fiber asphalt mastic revealed that FBF could effectively enhance the high-temperature rheological properties and low-temperature tensile properties of asphalt mastic compared with other fibers. FBF asphalt mastic improved the asphalt rutting factor by more than four times. The tensile fracture energy of fiber asphalt mastic was more than three times that of the corresponding asphalt. The reinforcement effect of BBF was poor; it was recommended to be broken up before use.

KEYWORDS

road engineering, basalt fiber, orthogonal experiment, fuzzy comprehensive evaluation method, fiber asphalt mastic properties

1 Introduction

Asphalt pavement has been widely used in highway engineering for its good performance in enhancing skid resistance, reducing noise, and excellent anti-friction performance (Zhu et al., 2020; Li L. et al., 2021; Zho et al., 2021; Yu et al., 2022; Li and Chen, 2023). With the rapid development of the economy, asphalt pavement is prone to damage such as high-temperature rutting, low-temperature cracking, water damage, and spalling (Zhang and Huang, 2019; Cheng et al., 2020; Ch et al., 2021; Yalghouzaghaj et al., 2021; Chen et al., 2023). Therefore, higher requirements have been put forward for the durability, crack resistance, and temperature stability of asphalt pavement materials (Pi et al., 2020; Long et al., 2022; Lu et al., 2022; Noorvand et al., 2022; Zhang et al., 2022; Zhang et al., 2023).

Basalt fiber is an economical and environmentally friendly inorganic material that has high tensile strength, chemical stability, and great resistance to temperature, corrosion, alkalies, and acids. Relevant literature has confirmed that compared with ordinary asphalt concrete and other types of fiber asphalt concrete, basalt fiber asphalt concrete has excellent high- and low-temperature performance, water stability, and fatigue resistance; the incorporation of basalt fiber can significantly improve the road performance of an asphalt mixture (Guo et al., 2021; Wu et al., 2022a; Cheng et al., 2022; Hui et al., 2022; Liang et al., 2022). Hence, it has been widely used to stabilize the mechanical properties of asphalt concrete. Li Z. et al. (2021) concluded that the optimal asphalt content of SBS-modified asphalt mixture with a basalt fiber content of 0.00%, 0.15%, 0.25%, and 0.35% was 4.90%, 5.05%, 5.15%, and 5.20%. The fiber was irregularly distributed in the mixture to form a three-dimensional network structure. Wu et al. (2021) focused on the experimental research on the performance of basalt fiber-modified asphalt mixture and showed that the optimal fiber weight content was 0.3%. Yang et al. (2023) found that the optimal dosages of granular lignin fiber (LF)-reinforced stone mastic asphalt mixture (SMA13), flocculent lignin fiber-reinforced SMA, and basalt fiber-reinforced SMA were 0.50 wt%, 0.45 wt%, and 0.50 wt%, respectively. Guo et al. (2020) conducted the Marshall stability test and wheel tracking test and confirmed that adding basalt fiber could improve several high-temperature indexes of asphalt mixture effectively. Pei et al. (2021) indicated that the inclusion of basalt fiber could improve crack resistance, slow the increase of displacement, and delay the fracture time of asphalt concrete. Lou et al. (2021) suggested that basalt fiber could increase the fatigue life, the change rate of dissipated energy, and the cumulative dissipated energy of the mixture. The addition of basalt fiber could obtain a better reinforcement effect than SBS-modified asphalt. Zhu et al. (2022) showed that the fatigue life of asphalt mixture increased with the inclusion of basalt fiber and diatomite. Adding basalt fiber and diatomite increased the fatigue life more than adding diatomite/basalt fiber. Jiu et al. (2023) manifested that basalt fiber could improve the dynamic stability, penetration strength, dynamic modulus index, and flow number of asphalt mixture significantly; it was an effective solution to the rutting deformation damage of asphalt pavement.

From the aforementioned studies, we know that many studies on basalt fiber-reinforced asphalt mixture have achieved remarkable results, but most mainly focus on the impact of fiber content or other fiber characteristics on the performance of the mixture (Wang et al., 2019; Etin et al., 2020; Kou et al., 2020). The asphalt mastic is the most essential and important parameter that needs to be taken into consideration in the design of the mixture and determines the properties of the mixture. However, relevant studies on basalt fiber-reinforced asphalt mastic are rare. Xie et al. (2022) studied the rheological properties of basalt fiber asphalt mastic and found that the rutting factor of basalt fiber asphalt mastic was higher than that of pure asphalt mastic, and the enhancement effect was more significant at high temperatures. Wu et al. (2022a) examined four kinds of basalt fibers (three short-cut fibers coated with different infiltration agents and one flocculated basalt fiber, noted as BF-A, BF-B, BFC, and FBF) to evaluate the effect of fibers on the rheological behavior of asphalt mastic. That study selected LF as a control and concluded that fibers improve the deformation resistance of asphalt mastic. Among them, BF-A and LF showed the most significant improvements in high- and low-temperature performance, respectively. The morphology of the fibers and the type of infiltration agent on the fiber surface affect the rheological properties of fiber asphalt mastic and lead to different effect mechanisms. Wu et al. (2022b) also found that after adding basalt fiber to asphalt mastic, the complex modulus of the mastic increased while the phase angle decreased. Moreover, the impregnating agents critically impacted the rheological properties of asphalt mastic. Gu et al. (2022) proposed that the asphalt mortars with type A basalt fiber present superior rheological performance at high and low temperatures, with an optimal fiber content of 2% and fiber length of 9 mm.

In summary, there is abundant research on basalt fiber asphalt mixture, but the research on the mechanical properties of basalt fiber asphalt mastic is still in the exploratory stage. The study of basalt fiber asphalt mastic composition has not been based on the need to understand its properties. Few studies have examined the influence of basalt fiber morphology on the mechanical properties of asphalt. The construction ratio of the basalt fiber asphalt mixture determines the reasonable range of fiber content, the filler–asphalt ratio, and the asphalt viscosity of fiber asphalt mastic. According to that, in this study, the optimal ratio of basalt fiber asphalt mastic suitable for asphalt mixture of different structure types was determined using the orthogonal experimental and fuzzy comprehensive evaluation (FCE) method. Subsequently, a series of laboratory tests (apparent viscosity test, penetration test, softening point test, ductility test, high-temperature rheological properties test, and low-temperature tensile test) were conducted to analyze the properties of basalt fiber asphalt mastic suitable for different structural types. Based on the optimal ratio of basalt fiber asphalt mastic, the influence of different fiber types on the properties of asphalt mastic was compared and analyzed. These findings are intended to provide a theoretical basis for the increased use and engineering application of basalt fiber in asphalt pavement.

2 Materials and schemes

2.1 Asphalt

The asphalts used were 90# matrix asphalt and SBS-modified asphalt, provided by Panjin Northern Asphalt Co., Ltd., located in Liaoning Province, China. The technical indexes of matrix asphalt and modified asphalt are shown in Tables 1, 2, respectively.

Tables 1 and 2 show that the two asphalts met the requirements of the Chinese specification of JTG E20-2011, Standard Test Methods of Bitumen and Bituminous Mixture for Highway Engineering (JTG E20, 2011). Furthermore, the SBS-modified asphalt met the Class I-C requirements in the specification.

2.2 Fiber

The basalt fiber used was the chopped basalt fiber produced by Jilin Tongxin Basalt Technology Co., Ltd., of Tonghua City in Jilin Province. Bundled basalt fiber (BBF), flocculated basalt fiber (FBF),

TABLE 1 Technical indexes and test data of 90# matrix asphalt.

Test item	Specification requirement	Test result	Test method
Penetration (25°C)/0.1 mm	80–100	88.70	T0604
Softening point/°C	≥44	45.30	T0606
Elongation (5 cm/min, 15°C)/cm	≥100	102.30	T0605
Apparent viscosity (135°C)/Pa·s	-	0.30	T0625
Flashpoint/°C	≥245	296	T0611
Asphalt density (15°C)/g·cm^{-3}	Measured record	1.019	T0603
After RTFOT			
Quality change/%	±0.8	−0.093	T0609
Residual penetration value ratio (25°C)/%	≥57	64.9	T0604
Residual ductility (5 cm/min, 15°C)	≥20	46.67	T0605

TABLE 2 Technical indexes and test data of SBS-modified asphalt.

Test item	Specification requirement	Test result	Test method
Penetration (25°C)/0.1 mm	60–80	66.70	T0604
Softening point/°C	≥55	55.90	T0606
Elongation (5 cm/min, 5°C)/cm	≥30	40.80	T0605
Apparent viscosity (135°C)/Pa·s	≤3	1.110	T0625
Flashpoint/°C	≥230	259	T0611
Asphalt density (15°C)/g·cm^{-3}	Measured record	1.026	T0603
After RTFOT			
Quality change/%	≤1.0	−0.066	T0609
Residual penetration value ratio (25°C)/%	≥60	66.9	T0604
Residual ductility (5 cm/min, 5°C)	≥20	23.6	T0605

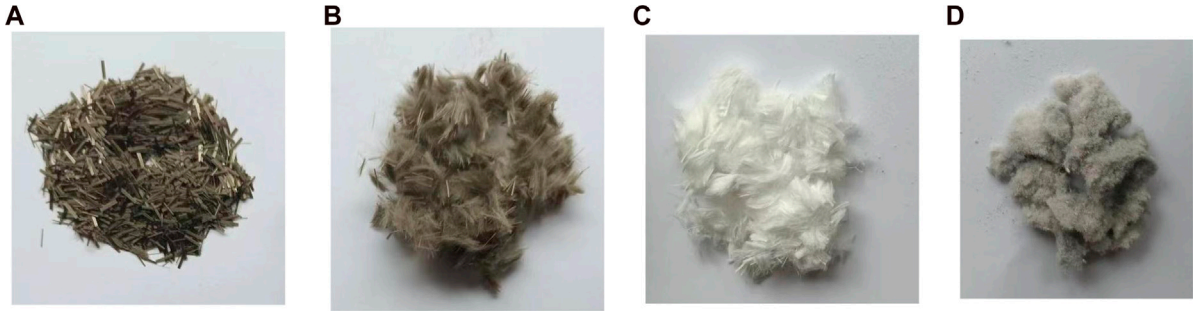

FIGURE 1
Images of different fibers: **(A)** BBF, **(B)** FBF, **(C)** PF, and **(D)** LF.

polyester fiber (PF), and LF were selected to study the influence of fiber morphology and fiber type on the properties of asphalt mastic. The morphology of each fiber is shown in Figure 1, and the technical indexes of each fiber are shown in Table 3.

2.3 Mineral powder

The mineral powder used was limestone mineral powder produced by Jilin Jiusheng Ecological Environment Technology

TABLE 3 Technical indexes of various fibers.

Fiber	Appearance	Diameter/μm	Length/mm	Density/g·cm^{-3}	Melting point/°C	Oil absorption rate/times
BBF	Golden brown, bunched	13	6	2.72	1450	0.774
FBF	Dark brown, monofilamentous	13	6	2.72	1450	4.339
LF	Light gray, loose and flocculent	43	0.8	1.23	230	6.206
PF	Milky white, bundled monofilament	20	6	1.39	220	4.786

Note: The oil absorption rate is the ability of fiber to absorb kerosene.

TABLE 4 Mineral powder performance indexes and test data.

Test item	Test result	Specification requirement	Test method
Apparent relative density/g·cm^{-3}	2.74	≥2.50	T0352
Water content/%	0.6	≤1	T0103
			Drying method
Appearance	Qualified	No agglomeration	-
Hydrophilic coefficient	0.63	<1	T0354
Plasticity index	3	<4	
Particle size range <0.6 mm/%	99.8	100	T0351
<0.15 mm/%	99.6	90–100	
<0.075 mm/%	99.4	75–100	

TABLE 5 Fiber content and filler–asphalt ratio of asphalt mastic corresponding to different asphalt mixture types.

Asphalt mixture				Asphalt mastic	
Mixture type	Optimal asphalt dosage (%)	Mineral powder dosage (%)	Suitable fiber content (%)	Filler–asphalt ratio	Fiber content (%)
SMA	5.60–5.84	10	0.4	1.71–1.79	6.80–7.10
AC	4.30–4.60	5	0.3	1.09–1.16	6.50–7.00
ATB	3.56–3.85	4	0.3	1.04–1.12	7.80–8.00

Co., Ltd., of Siping City in Jilin Province. In order to avoid the impact of variations in mineral powder size on the properties of asphalt mastic, a square-hole sieve with a pore size of 0.075 mm was selected to screen the mineral powder. Mineral powder components with a particle size of less than 0.075 mm were selected to ensure data stability. The technical indexes of mineral powder are shown in Table 4.

2.4 Orthogonal experiment design

To simulate the actual state of FBF in asphalt mixture, the fiber content and filler–asphalt ratio in asphalt mixture of different structural types were determined according to engineering empirical methods, as shown in Table 5.

Table 5 shows that the fiber content in different types of asphalt mixture ranged from 6.50% to 8.00%, and the filler–asphalt ratio ranged from 1.04 to 1.79. A trial test of fiber asphalt mastic was carried out based on Table 5 to determine the dosage range of each factor. When the fiber content was 3.5%, the phenomenon of fiber agglomeration occurred. Increasing the mixing temperature did not eliminate the phenomenon of fiber agglomeration, so the fiber content in asphalt mastic should not exceed 3.5%. Therefore, considering the engineering empirical data and trial tests, the fiber content of asphalt mastic was selected as 1%, 2%, and 3%. The filler–asphalt ratio ranged from 1.0 to 1.8. The apparent viscosities of 90# matrix asphalt and SBS-modified asphalt at 135°C were 0.30 Pa·s and 1.10 Pa·s, respectively. Therefore, the asphalt viscosity ranged from 0.30 Pa·s to 1.10 Pa·s.

TABLE 6 Basalt fiber asphalt mastic orthogonal experiment design.

Level	Factor A	Factor B	Factor C	Factor D
	Fiber content/%	Filler–asphalt ratio	Asphalt viscosity/Pa·s	Error
1	1.00	1.00	0.30	
2	2.00	1.40	0.70	
3	3.00	1.80	1.10	

FIGURE 2
Apparent viscosity instrument.

FIGURE 3
Different types of rotor.

The fiber content, filler–asphalt ratio, and asphalt viscosity were selected as three factors. The L9 (34) orthogonal array table (Table 6) was used to conduct a series of laboratory tests (apparent viscosity test, penetration test, softening point test, ductility test, DSR test, and low-temperature tensile test) to analyze the effects of fiber content, filler–asphalt ratio, and asphalt viscosity on the properties of fiber asphalt mastic. Furthermore, the FCE method was used to explore the optimal ratio of fiber asphalt mastic suitable for gap-graded and dense-graded asphalt mixtures with different factors.

3 Methods

3.1 Apparent viscosity test

The apparent viscosity test was conducted using an apparent viscosity instrument (Figure 2) according to the Chinese specification of JTG E20-2011 (T0619) (JTG E20, 2011). First, the molded fiber asphalt mastic was placed in the oven for 1.5 h to equilibrate to the test temperature. The segregation of fibers and mineral powder at high temperatures will affect the results of asphalt viscosity. The asphalt mastic was stirred with a thin steel wire to evenly disperse the fibers and mineral powder before placing it in the heating barrel equipped with a viscometer to avoid errors in results caused by segregation. During the test, different rotor types and rotor speeds were required to ensure that the torque was controlled within 10%–98%. When the test temperature was lower than 160°C, a 27# rotor was used; otherwise, a 21# rotor was used (Figure 3) to improve the accuracy of test results.

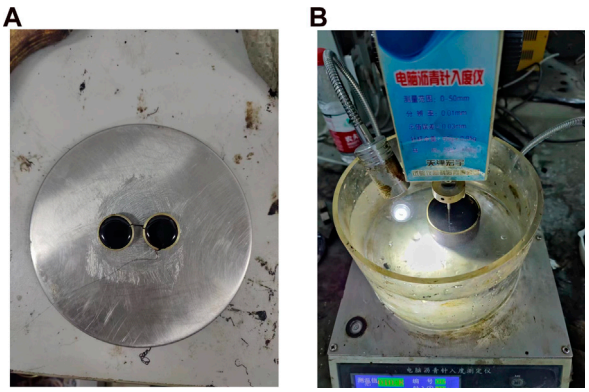

FIGURE 4
Penetration test: **(A)** prepared asphalt mastic in the tray and **(B)** penetration test.

3.2 Penetration test

A penetration test (Figure 4) was carried out in accordance with the requirements of the Chinese specification of JTG E20-2011 (T0604) (JTG E20, 2011). The sample tray was a copper tray with a diameter of 70 mm and a depth of 50 mm. The instrument used was the penetration meter, and the weight of the needle and pin linkage combination was 100 ± 0.05 g. During the test, the prepared asphalt mastic was added to the tray, cooled at room temperature for 2 h, and then transferred to a constant temperature water bath at 25°C ± 0.5°C for 2 h, after which the sample penetration was determined.

FIGURE 5
Softening point test.

FIGURE 7
Dynamic shear rheometer.

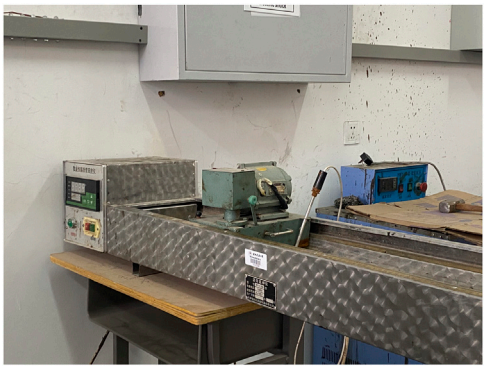

FIGURE 6
Asphalt ductility instrument.

3.3 Softening point test

Based on the Chinese specification of JTG E20-2011 (T0606) (JTG E20, 2011), the softening point test was conducted using the softening point instrument with a steel ball diameter of 9.53 mm and a mass of 3.5 ± 0.05 g, shown in Figure 5. During the test, the fiber asphalt mastic was slowly injected into the sample ring and then cooled for 30 min at room temperature. Any asphalt mastic higher than the sample ring was removed with a hot scraper, and then the sample was placed in the softening point instrument to determine the softening point of the sample.

3.4 Ductility test

According to the Chinese specification of JTG E20-2011 (T0605) (JTG E20, 2011), the ductility test was carried out using an asphalt ductility instrument (Figure 6). The test temperature was set at 5°C, and the tensile rate was 5 ± 0. 25 cm/min. Before the test, the sample was cooled at room temperature for not less than 1.5 h. Any asphalt mastic higher than the mold was removed with a hot scraper. Subsequently, the mold was placed with the bottom plate in the sink at the specified temperature and kept for 1.5 h.

3.5 High-temperature rheological property test

The dynamic shear rheological test was conducted using a dynamic shear rheometer (Figure 7) according to the Chinese specification JTG E20-2011 (T0628) (JTG E20, 2011). The complex shear modulus and phase angle of fiber asphalt mastic at 52°C, 58°C, 64°C, 70°C, and 76°C were obtained. The complex shear modulus and phase angle were used to characterize the viscoelastic properties of fiber asphalt mastic. The complex shear modulus includes both elastic and viscous parts; the larger the complex shear modulus, the greater the stiffness of the fiber asphalt mastic and the stronger the resistance to flow deformation. The phase angle is the relative index of elasticity and viscosity coefficient; the smaller the phase angle, the more the fiber asphalt mastic resembles a soft elastomer and the stronger its recovery ability after a strain.

3.6 Low-temperature tensile test

A low-temperature tensile test was used to study the low-temperature properties of fiber asphalt mastic based on the Chinese specification of JTG E20-2011 (T0629) (JTG E20, 2011). First, a fiber asphalt mastic plate sample with the size of 150 mm × 45 mm × 10 mm was prepared on a glass plate. After the sample was formed, the test temperature (−10°C, −20°C, −and 30°C) was held constant for 4 h. Subsequently, the DTS-30 universal testing machine was used for the low-temperature tensile test. The tensile rate was selected as 0.05 mm/s. When the ultimate tensile force of the sample was reached, the test was stopped. The test procedure is shown in Figure 8.

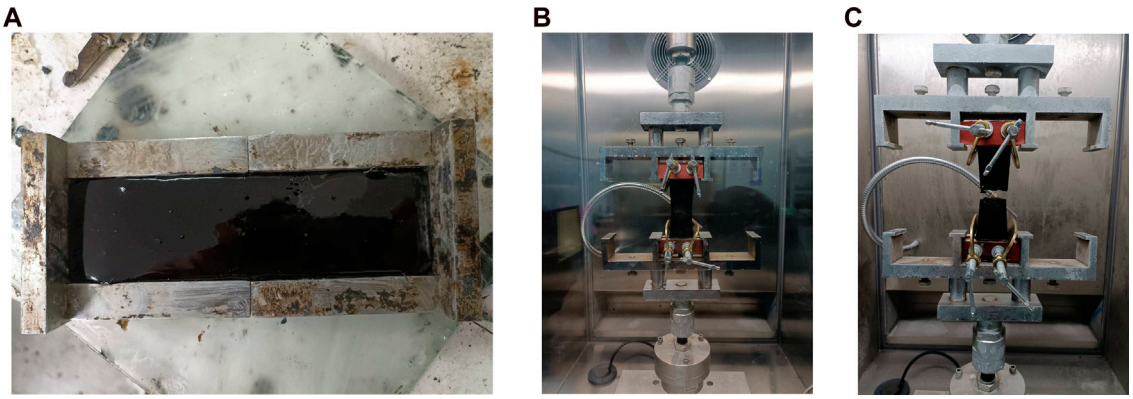

FIGURE 8
Low-temperature tensile test: **(A)** formed sample, **(B)** stretch stage, and **(C)** fracture stage.

TABLE 7 Orthogonal experiment results.

Test number	Apparent viscosity/Pa·s	Penetration/0.1 mm	Softening point/°C	Ductility/mm	Rutting factor	Fatigue factor	Low-temperature fracture energy/J
	135°C				64°C	64°C	−10°C
1	1.65	38.00	57.6	52.00	2.341	2.339	13.87
2	5.97	26.33	71.0	33.00	5.161	4.965	17.65
3	19.52	24.33	80.8	24.67	6.998	6.646	23.84
4	10.12	28.67	65.7	38.00	4.637	4.428	19.24
5	21.57	25.67	77.1	18.67	7.814	7.365	21.17
6	8.56	28.67	68.3	19.33	3.697	3.683	19.33
7	24.07	19.67	79.7	23.67	6.021	5.635	18.86
8	10.56	22.00	67.0	24.67	3.982	3.962	14.36
9	30.17	15.00	83.7	18.00	6.539	6.087	20.52

To comprehensively consider the tensile force and deformation of basalt fiber asphalt mastic when stretched at low temperatures, the low-temperature tensile fracture energy of asphalt mastic was used to comprehensively evaluate the crack resistance at low temperatures, which can be calculated by Equation 1.

$$W = \int_0^{\delta_0} F d\delta, \tag{1}$$

where F is the tensile force on the sample measured in kN, δ is the displacement of the sample at a certain moment measured in mm, and δ_0 is the maximum displacement of the sample measured in mm.

4 Results and discussion

4.1 The optimal ratio of FBF asphalt mastic

4.1.1 Orthogonal experiment results

The orthogonal experiment results of FBF asphalt mastic are shown in Table 7.

The range analysis and variance analysis were carried out on the results of the orthogonal experiment to examine the significance of the influence of fiber content, filler–asphalt ratio, and asphalt viscosity on various fiber asphalt mastic evaluation indexes. The calculation results are shown in Table 8.

Table 8 shows that the degree of influence of each factor on the apparent viscosity was C > A > B. Three factors had a significant effect on the penetration value. The degree of influence on penetration was A > C > B. The degree of influence on ductility was B > A > C, and the fiber content and filler–asphalt ratio were more significant. The degree of influence on the softening point, rutting factor, fatigue factor, and low-temperature fracture energy was C > B > A. Among them, asphalt viscosity had the most significant effect on the softening point, high-temperature rheological properties, and low-temperature tensile fracture energy of fiber asphalt mastic.

4.1.2 Fuzzy comprehensive evaluation results

4.1.2.1 Determination of index weight

To apply the FCE method to determine the optimal ratio of FBF asphalt mastic for different structural types, it was first

TABLE 8 Range analysis and variance analysis results.

Index	Range				Variance			
	A	B	C	D	A	B	C	D
Apparent viscosity/Pa·s	12.55	7.47	14.80	4.93	243.65	101.48	330.82	43.92
Penetration/0.1 mm	10.66	6.11	6.22	1.33	194.34	58.29	78.85	3.29
Softening point/°C	7.00	9.93	14.90	1.83	90.71	149.75	338.91	6.07
Ductility/mm	14.44	17.22	9.67	0.44	344.96	474.30	152.67	32.30
Rutting factor	0.68	1.41	3.60	0.60	0.78	3.74	19.67	0.55
Fatigue factor	0.58	1.34	3.22	0.50	0.60	3.47	15.66	0.38
Low-temperature fracture energy/J	2.00	3.90	5.44	0.63	6.43	27.67	45.01	0.69

TABLE 9 Weight of the FBF asphalt mastic index.

Structure type	Viscosity/ Pa·s	Penetration/ 0.1 mm	Softening point/°C	Ductility/ mm	Fatigue factor	Rutting factor	Low-temperature fracture energy/J
Gap-graded	0.13	0.14	0.15	0.14	0.16	0.12	0.16
Dense-graded	0.06	0.03	0.10	0.19	0.26	0.23	0.13

necessary to determine the weight of each index. To determine the weight value, first, the entropy weight method was used to analyze the weights of nine groups of tests on seven indexes of basalt fiber-reinforced asphalt mastic. However, the entropy weight method does not subjectively assign the importance of the index, reducing the influence of subjectivity on the decision-making. The entropy weight method does not consider the interaction between indexes, so it cannot fully consider the actual importance of each index. Thus, taking the weights of each index determined by the entropy weight method as a reference, the opinions of 30 experts were solicited on the influence of each index on the performance of basalt fiber-reinforced asphalt mastic suitable for different structural asphalt mixtures. Finally, the opinions of the experts were summarized, and the weight values of each index were averaged to obtain the final weight value. The final weight value of the fiber asphalt mastic index is shown in Table 9.

4.1.2.2 Acquisition of the evaluation matrix

The evaluation matrix was obtained by evaluating the degree to which each factor contributes to the evaluation matrix. In this paper, the evaluation matrix was determined by the membership function, which is the key to FCE and a measure of conceptual proximity. First, the fuzzy distribution formed by the experimental results was compared with the given membership functions, and then the membership function form was reasonably selected. The fuzzy distributions of the orthogonal experiment results of each index in this paper are similar to the normal distribution function. Meanwhile, considering that the medium value of each index had a greater influence on satisfaction, the previous and late values had little effect, and their properties were also similar to the normal distribution function. Therefore, the normal distribution function was taken as the membership function of the index. The index can be divided into two types, small and large, depending on whether a smaller index value is better or a larger index value is better.

$$f(x) = \begin{cases} 1, & x \le a, \\ e^{-\left(\frac{x-a}{\sigma}\right)^2}, & a < x, \end{cases} \tag{2}$$

$$f(x) = \begin{cases} 0, & x \le a, \\ 1 - e^{-\left(\frac{x-a}{\sigma}\right)^2}, & a < x. \end{cases} \tag{3}$$

Equations 2 and 3 are the descending half-normal distribution functions and the ascending half-normal distribution functions, respectively, and are suitable for the small index and the large index, respectively. $f(x)$ is the satisfaction function value. For a small index, if $x \le a$, it is considered completely acceptable, that is, completely satisfied. If $a < x$, the satisfaction presents a normal downward trend with an increasing index value. A large index is the opposite of a small index. Among the various indexes, the penetration and fatigue factor indexes are relatively small, and the other indexes are relatively large.

The satisfaction function value of the orthogonal experiment results of each index can be calculated by the membership function. The satisfaction function of each index forms the evaluation matrix shown in Table 10, that is, the evaluation matrix of each fiber asphalt mastic index.

4.1.2.3 Comprehensive satisfaction

Comprehensive satisfaction is the contribution of each index value in the orthogonal experiment to the concept of satisfaction. In this paper, the weighted arithmetic average shown in Equation 4 was used to obtain the comprehensive satisfaction index (Su and Yao, 2004).

TABLE 10 Evaluation matrix of the FBF asphalt mastic index.

Index	1	2	3	4	5	6	7	8	9
Viscosity/Pa·s	0.000	0.208	0.982	0.592	0.993	0.450	0.998	0.629	1.000
Penetration/0.1 mm	0.000	0.040	0.101	0.011	0.059	0.008	0.636	0.322	1.000
Softening point/°C	0.000	0.937	1.000	0.635	0.997	0.828	0.999	0.743	1.000
Ductility/mm	1.000	0.867	0.329	0.972	0.004	0.016	0.250	0.329	0.000
Fatigue factor	1.000	0.046	0.000	0.142	0.000	0.446	0.008	0.308	0.002
Rutting factor	0.000	0.939	0.999	0.838	1.000	0.446	0.948	0.438	0.993
Low-temperature fracture energy/J	0.000	0.738	1.000	0.933	0.993	0.939	0.904	0.022	0.984

TABLE 11 Comprehensive satisfaction of the orthogonal experiment.

Test number	1	2	3	4	Comprehensive satisfaction	
					Gap-graded	Dense-graded
1	1 (1%)	1 (1.0)	1 (90#)	1	0.260	0.420
2	1 (1%)	2 (1.4)	2 (90# + SBS)	2	0.568	0.623
3	1 (1%)	3 (1.8)	3 (SBS)	3	0.658	0.614
4	2 (2%)	1 (1.0)	2 (90# + SBS)	3	0.610	0.656
5	2 (2%)	2 (1.4)	3 (SBS)	1	0.606	0.551
6	2 (2%)	3 (1.8)	1 (90#)	2	0.461	0.454
7	3 (3%)	1 (1.0)	3 (SBS)	2	0.701	0.592
8	3 (3%)	2 (1.4)	1 (90#)	3	0.395	0.372
9	3 (3%)	3 (1.8)	2 (90# + SBS)	1	0.737	0.577

$$f(B_i) = \sum_{j=1}^{n} w_j f_{A_j}(x_{ij}), i = 1, 2.....m, \quad (4)$$

where $f(B_i)$ is the comprehensive satisfaction of the ith test, w_j is the weight vector of the index, and $f_{Aj}(x_{ij})$ is the satisfaction value of the index. The comprehensive satisfaction of each group of orthogonal experiments shown in Table 11 can be obtained using Equation 4.

The range analysis and variance analysis were performed on the comprehensive satisfaction. The results are displayed in Table 12.

Table 12 shows that the asphalt viscosity has the most significant effect on the properties of FBF asphalt mastic, followed by the fiber content and the filler–asphalt ratio. For the gap-graded asphalt mixture, the highest comprehensive satisfaction score of fiber asphalt mastic was obtained by the combination of A3B3C3: when the fiber content was 3%, the filler–asphalt ratio was 1.8, and the asphalt viscosity was 1.1 Pa·s. That is to say, to obtain the asphalt mastic with the best properties for a gap-graded asphalt mixture, it is necessary to use more fiber content, more filler, and modified asphalt. For the dense-graded asphalt mixture, the fiber asphalt mastic with the combination of A2B1C2 has the highest comprehensive satisfaction score when the fiber content, filler–asphalt ratio, and asphalt viscosity were 2%, 1.0, and 0.7 Pa·s, respectively. For the dense-graded structure, fewer quantities of fiber and filler are needed, appropriately increasing the viscosity of the asphalt can further improve the properties of the asphalt mixture.

TABLE 12 Multi-index comprehensive satisfaction analysis of FBF asphalt mastic.

Structure type	Factor	A	B	C	D
Gap-graded	Mean 1	1.4860	1.5710	1.1160	1.6030
	Mean 2	1.6780	1.5700	1.9150	1.7300
	Mean 3	1.8320	1.8550	1.9650	1.6630
	Range R	0.1150	0.0950	0.2830	0.0420
	Variance	0.0201	0.0181	0.1514	0.0027
	F-value	7.4200	6.6700	55.970	1.0000
Dense-graded	Mean 1	1.6570	1.6680	1.2450	1.5480
	Mean 2	1.6610	1.5450	1.8550	1.6680
	Mean 3	1.5400	1.6450	1.7570	1.6420
	Range R	0.0400	0.0410	0.2030	0.0400
	Variance	0.0031	0.0028	0.0716	0.0027
	F-value	1.1600	1.0600	26.650	1.0000

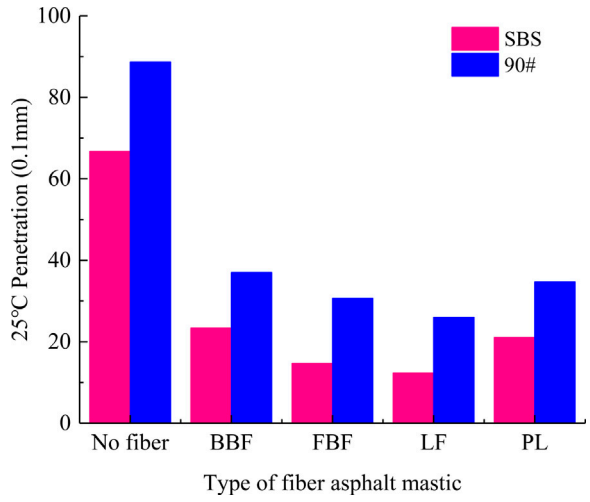

FIGURE 9
Penetration of various fiber asphalt mastics.

4.2 Effect of various fibers on asphalt mastic properties

BBF, FBF, PF, and LF were selected for comparative experiments to study the effect of different types of fiber on the properties of asphalt mastic. The optimal ratio of FBF asphalt mastic was selected as the optimal ratio of different types of fiber asphalt mastic. That is, for 90# matrix asphalt, the fiber content was 2%, and the filler–asphalt ratio was 1.0. For SBS-modified asphalt, the fiber content and filler–asphalt ratio were 3% and 1.8, respectively.

4.2.1 Effect of fiber on penetration

The penetration test results of four fiber asphalt mastics are shown in Figure 9. SBS-modified asphalt was taken as an example. The incorporation of BBF has a weaker effect on penetration than FBF; the improvement of asphalt hardness was not obvious. The reason is that BBF cannot be completely dispersed in asphalt. During the penetration test, the position of the needle is random; there may be no fiber at the penetration position or there may be fibers, and the two conditions result in different penetration values. The inclusion of FBF significantly improves the asphalt hardness because it can be completely dispersed in asphalt to form a continuous network structure, forming a "homogeneous" fiber asphalt mastic. The penetration value of the LF asphalt mastic was the smallest. The reason is that LF has a good ability to adsorb asphalt so that free asphalt can be converted into structural asphalt that adheres to the surface of the fiber. The macroscopic manifestation of the increased proportion of structural asphalt is the increase in hardness. The variation of penetration of the 90# matrix asphalts with different fibers is similar to that of SBS-modified asphalt.

4.2.2 Effect of fiber on the softening point

Figure 10 shows that the effect of fiber on the softening point of two different structural fiber asphalt mastics was the same. The LF asphalt mastic had the highest softening point, followed by the FBF asphalt mastic. The softening points of the BBF and PF asphalt mastics were similar. The reason is that the structural characteristics of LF make it better at adsorbing asphalt, which increases the viscosity of the fiber asphalt mastic and improves the softening point. However, the softening point of the BBF asphalt mastic was lower than that of the FBF asphalt mastic because the bundle form cannot be completely dispersed and cannot fully contribute to adsorption and stabilization.

4.2.3 Effect of fiber on the ductility

As Figure 10 indicates, incorporating fiber sacrifices the ductility of asphalt mastic. Fiber asphalt mastic is a typical viscoelastic plastic material. Fiber increases the viscosity of asphalt mastic, which leads to an increase in brittleness. The influence of BBF on the ductility of asphalt mastic is smaller than that of FBF. The fracture position of BBF asphalt mastic is not directly broken; the damage starts at a place with fewer fibers. When the displacement reaches a certain value, the fibers fail, and the sample can only rely on the matrix asphalt's own ductility. In contrast, FBF is more completely dispersed in asphalt, which improves the hardness and high-temperature stability of asphalt mastic but reduces ductility and deformation ability. The ductility of the LF asphalt mastic is the smallest. Compared with FBF asphalt mastic, fiber can be seen in the cross section. This fiber indicates that FBF serves as a reinforcement and can better transmit a load under stress, avoiding the concentration of stress and increasing the ductility and deformation ability of the asphalt mastic.

4.2.4 Effect of fiber on high-temperature rheological properties

The curves of the rutting factor with temperature are shown in Figure 11. Although the rutting factors of different fiber asphalt mastic are different, the changes in the rutting factor with temperature are consistent and decrease with the increase in temperature. Temperature has a significant effect on the high-temperature rheological properties of fiber asphalt mastic. The rutting factor of fiber asphalt mastic is significantly improved compared with asphalt mastic without fibers. Over a temperature range from 52°C to 76°C, the incorporation of fibers significantly improved the rutting factor. The reason is that fibers have a good dispersion effect in asphalt mixture. Asphalt adheres to the fiber surface because of its good adsorbability, reducing the amount of free asphalt in the asphalt mastic and improving the viscosity of fiber asphalt mastic. Fibers can also form a three-dimensional network in an asphalt mixture, which also improves the resistance to high-temperature deformation.

The amount of rutting factor improvement of the four fiber asphalt mastics from largest to smallest was as follows LF > FBF > PF > BBF. The enhancement effect of LF and FBF on high-temperature properties was similar, but the enhancement effect of LF was slightly better than that of FBF. LF and FBF had the largest enhancement on the high-temperature rheological properties of asphalt mastic at 52°C. FBF could exert its own ability to adsorb asphalt better than BBF; the good absorption capacity significantly improved the high-temperature performance. Among the fiber asphalt mastic suitable for gap-graded asphalt mixture, the rutting factors of LF asphalt mastic and FBF asphalt mastic increased 4.58 times and 4.14 times, respectively, compared with SBS-modified asphalt. In the fiber asphalt mastic suitable for a

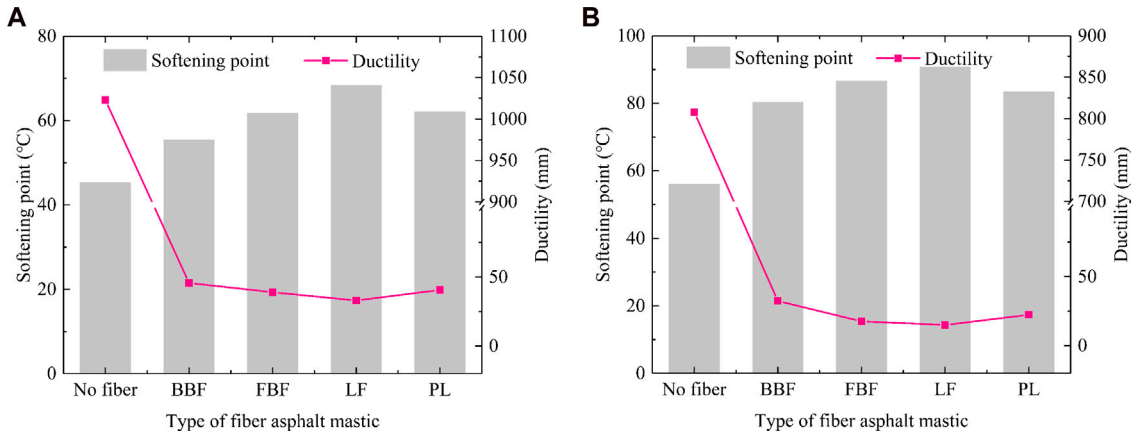

FIGURE 10
Softening point and ductility values of various fiber asphalt mastics in different structures: **(A)** gap-graded fiber asphalt mastic and **(B)** dense-graded fiber asphalt mastic.

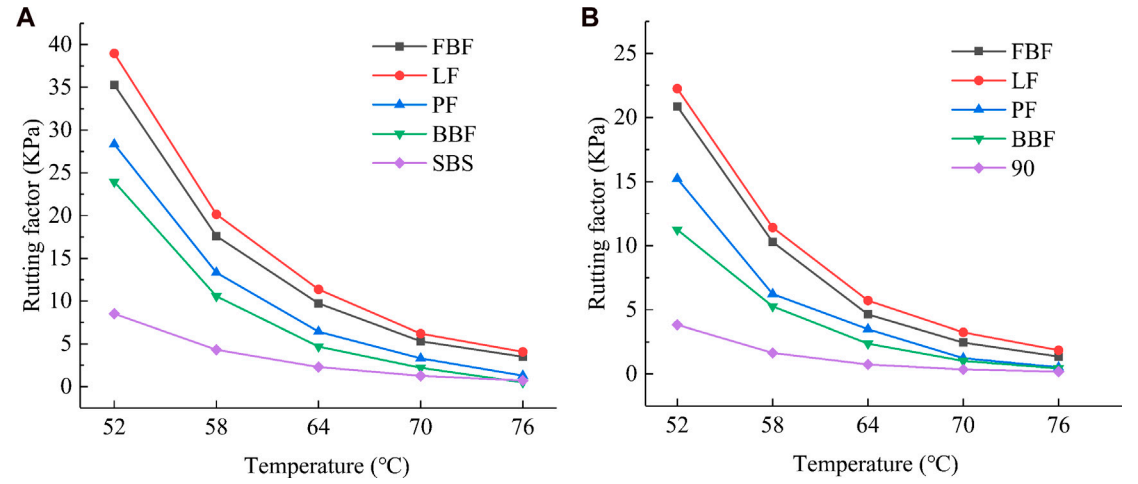

FIGURE 11
High-temperature rheological properties of various fiber asphalt mastics in different structures: **(A)** gap-graded fiber asphalt mastic and **(B)** dense-graded fiber asphalt mastic.

dense-graded asphalt mixture, the rutting factors of LF asphalt mastic and FBF asphalt mastic increased 5.81 times and 5.44 times, respectively, compared with 90# matrix asphalt.

4.2.5 Effect of fiber on low-temperature tensile properties

The low-temperature tensile fracture energy is an index to evaluate the low-temperature tensile properties of fiber asphalt mastic. The curves of low-temperature tensile fracture energy with temperature are shown in Figure 12. The low-temperature fracture energies of different fiber asphalt mastics vary, but they all decrease with a decrease in temperature. The anti-cracking ability of fiber asphalt mastic at low temperatures was significantly improved compared to that of no fiber. Over a temperature range from −10°C to −30°C, adding fiber significantly improved the anti-cracking ability of asphalt binder. The main reason is that the incorporation of fiber and mineral powder, as well as the good oil absorption capacity of fiber, increases the proportion of structural asphalt. Therefore, the viscosity of the asphalt binder increased, leading to the increase of the low-temperature ultimate tensile force. With the decrease in temperature, the ultimate tensile force increased, and the maximum displacement at failure decreased, resulting in the decrease of low-temperature tensile fracture energy.

FBF has the best effect on improving the low-temperature fracture energy of fiber asphalt mastic. FBF had better tensile properties than LF, greatly increasing the ultimate tensile force at break. The improving effect of LF and PF was not significant. BBF did not exert its own ability to adsorb asphalt because of its poor dispersion degree, so the improvement of ultimate breaking tensile force was limited compared with FBF.

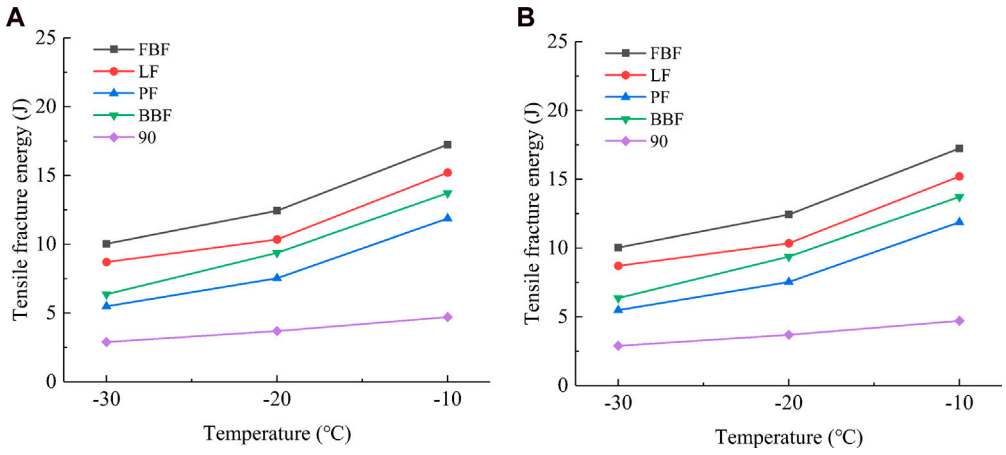

FIGURE 12
Low-temperature tensile fracture energy of various fiber asphalt mastics in different structures: **(A)** gap-graded fiber asphalt mastic and **(B)** dense-graded fiber asphalt mastic.

In the gap-graded asphalt mixture, the tensile fracture energy of FBF asphalt mastic at −10°C, −20°C, and −30°C was 3.08 times, 3.64 times, and 3.58 times that of SBS-modified asphalt, respectively. In the dense-graded asphalt mixture, the tensile fracture energy of FBF asphalt mastic at −10°C, −20°C, and −30°C was 3.66 times, 3.36 times, and 3.47 times that of 90 # matrix asphalt, respectively.

Fiber asphalt mastic mainly exerts tensile resistance at low temperatures in the gap-graded asphalt mixture, which makes up for the problem of insufficient low-temperature properties. However, the dense-graded asphalt mixture has good high-temperature rheological properties. The incorporation of fiber further enhances high-temperature rheological properties. In contrast, asphalt mixtures have more demanding requirements for the low-temperature properties of fiber asphalt mastics. FBF has a good effect on the high- and low-temperature properties of asphalt mastic due to its good oil absorption ability and excellent tensile strength.

5 Conclusion

1. An orthogonal experiment using the FCE method examined different construction ratios of different basalt fiber asphalt mixtures and concluded that the asphalt viscosity has the greatest influence on the comprehensive performance of basalt asphalt mastic, followed by the filler–asphalt ratio and the basalt fiber content.
2. The optimal ratio of FBF asphalt mastic suitable for gap-graded asphalt mixture is a fiber content of 3%, a filler–asphalt ratio of 1.8, and an asphalt viscosity of 1.1 Pa·s. The optimal ratio suitable for a dense-graded asphalt mixture is a fiber content, filler–asphalt ratio, and asphalt viscosity of 2%, 1.0, and 0.7 Pa·s, respectively.
3. Within 3% fiber content, for a gap-graded asphalt mixture, higher fiber content and more filler can improve the properties of asphalt mixtures. Fewer quantities of fibers and fillers are needed for a dense-graded asphalt mixture, appropriately increasing the viscosity of asphalt can improve the properties of a gap-graded asphalt mixture.
4. The test results of different types of fiber asphalt mastic showed that FBF could effectively enhance the high- and low-temperature properties of asphalt mastic while increasing the rutting factor by more than four times and the tensile fracture energy by more than three times.

Data availability statement

The original contributions presented in the study are included in the article/Supplementary Material; further inquiries can be directed to the corresponding author.

Author contributions

CS: conceptualization, methodology, resources, and writing–review and editing. JW: formal analysis, methodology, and writing–original draft. SS: resources, validation, and writing–review and editing. DL: investigation and writing–original draft. LX: investigation and writing–review and editing. SZ: data curation and writing–original draft.

Acknowledgments

The authors would like to thank the technicians from all the institutions involved in this work who contributed to achieving this study's objectives. The authors would like to thank the reviewers for their constructive suggestions and comments to improve the quality of the paper.

Conflict of interest

Author JW was employed by CCCC Comprehensive Planning and Design Institute Co., Ltd.

The remaining authors declare that the research was conducted in the absence of any commercial or financial relationships that could be construed as a potential conflict of interest.

Publisher's note

References

Cheraghian, G., and Wistuba, M. P. (2021). Effect of fumed silica nanoparticles on ultraviolet aging resistance of bitumen. *Nanomaterials* 11, 454. doi:10.3390/nano11020454

Chen, X., Ren, D. Y., Tian, G. S., Xu, J., Ali, R., and Ai, C. F. (2023). Investigation on moisture damage resistance of asphalt pavement in salt and acid erosion environments based on Multi-scale analysis. *Constr. Build. Mater.* 366, 130177. doi:10.1016/j.conbuildmat.2022.130177

Cheng, P. J., Yi, J. Y., Guo, S. H., Pei, Z. S., and Feng, D. C. (2022). Influence of fiber dispersion and distribution on flexural tensile properties of asphalt mixture Based on finite element simulation. *Constr. Build. Mater.* 352, 128939. doi:10.1016/j.conbuildmat.2022.128939

Cheng, Y., Li, H., Wang, W., Li, L., and Wang, H. (2020). Laboratory evaluation on the performance degradation of styrene-butadiene-styrene-modified asphalt mixture reinforced with basalt fiber under freeze-thaw cycles. *Polymers* 12, 1092. doi:10.3390/polym12051092

Etin, A., Evirgen, B., Karsliolu, A., and Tuncan, A. (2020). The effect of basalt fiber on the performance of stone mastic asphalt. *Period. polytech-civ.* 65, 299–308. doi:10.3311/PPci.14190

Gu, Q. L., Kang, A. H., Li, B., Xiao, P., and Ding, H. (2022). Effect of fiber characteristic parameters on the high and low temperature rheological properties of basalt fiber modified asphalt mortar. *Case Stud.* 17, e01247. doi:10.1016/j.cscm.2022.e01247

Guo, F. C., Li, R., Lu, S. H., Bi, Y. Q., and He, H. Q. (2020). Evaluation of the effect of fiber type, length, and content on asphalt properties and asphalt mixture performance. *Materials* 13, 1556. doi:10.3390/ma13071556

Guo, Q. L., Chen, Z. P., Liu, P. F., Li, Y. M., Hu, J. X., Gao, Y., et al. (2021). Influence of basalt fiber on mode i and ii fracture properties of asphalt mixture at medium and low temperatures. *Theor. Appl. Fract. Mech.* 112, 102884. doi:10.1016/j.tafmec.2020.102884

Hui, Y. X., Men, G. Y., Xiao, P., Tang, Q., Han, F. Y., Kang, A. H., et al. (2022). Recent advances in basalt fiber reinforced asphalt mixture for pavement applications. *Materials* 15, 15196826. doi:10.3390/ma15196826

Jiu, X. Y., Wang, Y., Wu, Z. G., Xiao, P., and Kang, A. H. (2023). High-temperature performance evaluation of asphalt mixture by adding short-chopped basalt fiber. *Buildings* 13, 13020370. doi:10.3390/buildings13020370

JTG E20 (2011). *Standard test methods of bitumen and bituminous mixture for highway engineering*. Beijing, China: China Communications Press.

Kou, C., Wu, X., Xiao, P., Liu, Y., and Wu, Z. (2020). Physical, rheological, and morphological properties of asphalt reinforced by basalt fiber and lignin fiber. *Materials* 13, 13112520. doi:10.3390/ma13112520

Li, L., Zhang, Z., Wang, Z., Wu, Y., and Zhang, Y. (2021a). Coupled thermo-hydro-mechanical response of saturated asphalt pavement. *Constr. Build. Mater.* 283, 122771. doi:10.1016/j.conbuildmat.2021.122771

Li, Q., and Chen, Z. X. (2023). Numerical analysis and conversion of dynamic and static deflection of asphalt pavement under FWD loading. *Constr. Build. Mater.* 367, 129513. doi:10.1016/j.conbuildmat.2022.129513

Li, Z., Guo, T., Chen, Y., Jin, L., Xu, Q., Wang, J., et al. (2021b). Study on properties of drainage SBS modified asphalt mixture with fiber. *Adv. Civ. Eng.* 2021, 1–17. doi:10.1155/2021/7846499

Liang, R. W., Yu, W., and Luo, Z. J. (2022). Laboratory investigation on pavement performance of basalt fiber-reinforced asphalt mixture under the coupling effect of freeze-thaw cycles and aging. *Front. Mater.* 9, 930056. doi:10.3389/fmats.2022.930056

Long, A., Sun, X. J., Yu, Z. P., Zhang, B. Y., Zhang, G. L., Huang, P. J., et al. (2022). Experimental study and mechanism analysis on the basic mechanical properties of hydraulic basalt fiber asphalt concrete. *Mater. Struct.* 55, 161. doi:10.1617/s11527-022-02001-y

Lou, K. K., Wu, X., Xiao, P., and Zhang, C. (2021). Investigation on fatigue performance of asphalt mixture reinforced by basalt fiber. *Materials* 14, 5596. doi:10.3390/ma14195596

Lu, P. Z., Ma, Y. H., Ye, K., and Huang, S. M. (2022). Analysis of high-temperature performance of polymer-modified asphalts through molecular dynamics simulations and experiments. *Constr. Build. Mater.* 350, 128903. doi:10.1016/j.conbuildmat.2022.128903

Noorvand, H., Mamlouk, M., and Kaloush, K. (2022). Evaluation of optimum fiber length in fiber-reinforced asphalt concrete. *J. Mater. Civ. Eng.* 34, 04021494. doi:10.1061/(asce)mt.1943-5533.0004128

Pei, Z., Lou, K., Kong, H., Wu, B., Wu, X., Xiao, P., et al. (2021). Effects of fiber diameter on crack resistance of asphalt mixtures reinforced by basalt fibers based on digital image correlation Technology. *Materials* 14, 7426. doi:10.3390/ma14237426

Pirmohasphalt, S., Shokorlou, Y. M., and Amani, B. (2020). Laboratory investigations on fracture toughness of asphalt concretes reinforced with carbon and kenaf fibers. *Eng. Fract. Mech.* 226, 106875. doi:10.1016/j.engfracmech.2020.106875

Su, H. H., and Yao, Z. J. (2004). Fuzzy analysis method for multi-index orthogonal test. *J. Nanjing Univ. Aeronaut. Astronaut.* 36, 29–33. doi:10.16356/j.1005-2615.2004.01.006

Wang, X., He, J., Mosallam, A. S., Li, C., and Xin, H. (2019). The effects of fiber length and volume on material properties and crack resistance of basalt fiber reinforced concrete (BFRC). *Adv. Mater. Sci. Eng.* 2019, 1–17. doi:10.1155/2019/7520549

Wu, B., Pei, Z., Luo, C., Xia, J., Chen, C., and Kang, A. (2022a). Effect of different basalt fibers on the rheological behavior of asphalt mastic. *Constr. Build. Mater.* 318, 125718. doi:10.1016/j.conbuildmat.2021.125718

Wu, B. W., Pei, Z. H., Xiao, P., and Lou, K. K. (2022b). Evaluation of the interfacial interaction ability between basalt fibers and the asphalt mastic. *Materials* 15, 15228209. doi:10.3390/ma15228209

Wu, B., Wu, X., Xiao, P., Chen, C., Xia, J., and Lou, K. (2021). Evaluation of the long-term performances of SMA-13 containing different fibers. *Appl. Sci.* 11, 5145. doi:10.3390/app11115145

Xie, T. T., Zhao, K., and Wang, L. B. (2022). Reinforcement effect of different fibers on asphalt mastic. *Materials* 15, 15238304. doi:10.3390/ma15238304

Yalghouzaghaj, M. N., Mikaeil, N., Sarkar, A., Hamedi, G. H., and Hayati, P. (2021). Application of the surface free energy method on the mechanism of low-temperature cracking of asphalt mixtures. *Constr. Build. Mater.* 268, 121194. doi:10.1016/j.conbuildmat.2020.121194

Yang, S. Y., Zhou, Z. G., and Li, K. (2023). Influence of fiber type and dosage on tensile property of asphalt mixture using direct tensile test. *Materials* 16, 16020822. doi:10.3390/ma16020822

Yu, X., Luo, R., and Huang, T. (2022). Moisture content prediction model of asphalt mixture based on dielectric properties. *J. Mate. Civ. Eng.* 353, 129042. doi:10.1061/(ASCE)MT.1943-5533.0004155

Zhang, G. H., Wu, H. N., Li, P., Qiu, J. H., and Nian, T. F. (2022). Pavement properties and predictive durability analysis of asphalt mixture. *Polymers* 14, 14040803. doi:10.3390/polym14040803

Zhang, J. Q., Wang, W. C., Liu, J. Z., Wang, S. Y., Qin, X. C., and Yu, B. (2023). Pavement performance and ice-melting characteristics of asphalt mixture incorporating slow-release deicing agent. *Buildings* 13, 13020306. doi:10.3390/buildings13020306

Zhang, Q. L., and Huang, Z. Y. (2019). Investigation of the microcharacteristics of asphalt mastics under dry-wet and freeze-thaw cycles in a coastal salt environment. *Materials* 12, 2627. doi:10.3390/ma12162627

Zhong, Y., Gao, Y., Zhang, B., Li, S., Cui, H., Li, X., et al. (2021). Experimental study on the dielectric model of common asphalt pavement surface materials based on the L-R model. *Adv. Civ. Eng.* 2021, 1–8. doi:10.1155/2021/6667101

Zhu, C. F., Luo, H. J., Tian, W., Teng, B. B., Qian, Y. M., Ai, H. X., et al. (2022). Investigation on fatigue performance of diatomite/basalt fiber composite modified asphalt mixture. *Polymers* 14, 14030414. doi:10.3390/polym14030414

Zhu, J. Q., Ma, T., Fan, J., Fang, Z., and Zhou, Y. (2020). Experimental study of high modulus asphalt mixture containing reclaimed asphalt pavement. *J. Clean. Prod.* 263, 121447. doi:10.1016/j.jclepro.2020.121447